

# A High-Efficiency Radial Flux Generator Using Finemet and Soft Magnetic Composite Materials: Performance and Techno-Economic Comparison with Conventional Aerospace Designs

Research Paper

Roby Mohajon<sup>1,\*</sup>, Abu Talha Haque Miah<sup>1</sup>, Nur Mohammad<sup>2</sup>

<sup>1</sup>Department of Electrical and Electronic Engineering, Barisal Engineering College, University of Dhaka, North Durgapur, Barisal, 8200, Bangladesh

<sup>2</sup>Chittagong University of Engineering and Technology, Chittagong, Bangladesh

Received: 14 October, 2025; Received in the revised form: 27 November, 2025; Accepted: 15 January, 2026

**Abstract:** The demand for lightweight, thermally stable, and energy-efficient power systems in aerospace applications has prompted the investigation of advanced magnetic materials beyond traditional alloys, such as Hiperco 50. This study aims to address the limitations of high core loss, poor efficiency, and thermal instability in conventional aerospace generators. A high-speed (10,000 RPM, 500 Hz) radial flux permanent magnet generator (RFPMG) was designed using Finemet as the stator material, soft magnetic composites (SMC) for the rotor, and Litz wire windings to minimise eddy current and copper losses. Electromagnetic and thermal simulations were conducted using ANSYS Maxwell and Motor-CAD to ensure adherence to aerospace standards (IEC 60034-1, SAE ARP4990, IEEE 1812-2014). The results indicate that the proposed Finemet–SMC design achieves a 59% increase in output power (7.49 kW vs. 4.71 kW), an 11% improvement in efficiency (96.19% vs. 86.47%), and a 60% reduction in total losses, with stator and winding temperatures reduced by up to 45%. The torque ripple decreased by 44%, ensuring a smoother performance. These findings demonstrate that the proposed configuration not only surpasses standard aerospace requirements but also establishes a lightweight, cost-effective, and sustainable generator design suitable for next-generation hybrid and electrified aircraft propulsion systems.

**Keywords:** *thermal analysis • energy efficiency • light weight • radial flux generator • fuel saving*

## 1. Introduction

The growing emphasis on environmental sustainability and decarbonisation in the aviation industry has necessitated the development of lightweight, energy-efficient and thermally stable electrical systems. Electrified propulsion technologies, such as More Electric Aircraft (MEA), hybrid-electric systems and urban air mobility (UAM), require next-generation generators capable of ultra-high-speed operation under stringent mechanical and thermal constraints. The electrification of propulsion systems is a crucial step towards achieving sustainable and carbon-neutral flights across aerospace sectors. Traditional aerospace generators, which are constructed with laminated silicon steel cores and bulk copper windings, are inadequate for high-speed operational requirements because of excessive core losses, eddy current heating and limited heat dissipation. Consequently, ultra-high-speed generators (UHGs) operating above 10,000 RPM have garnered significant interest owing to their compact structure and high-power density, although they encounter challenges, such as thermal management, mechanical stress and electromagnetic efficiency (Huynh et al., 2005; Ismagilov et al., 2020; Wang et al., 2025).

Finemet, a nanocrystalline Fe–Si–B–Nb–Cu alloy, was employed as the stator material owing to its low core loss, high magnetic permeability and superior thermal stability. The rotor is composed of soft magnetic composites

\* Email: [robymohajon@gmail.com](mailto:robymohajon@gmail.com)

(SMCs) – materials with over 97% pure iron particles coated for electrical insulation, offering isotropic magnetic behaviour and high resistivity, which effectively minimises eddy current losses (Wang et al., 2025). Litz wire windings, made of 29 American Wire Gauge (AWG) copper strands, are utilised to reduce the AC resistance and mitigate skin and proximity effects, ensuring improved electromagnetic control and reduced copper loss at high frequencies (Shen et al., 2018; Sirimanna et al., 2022; Thangaraju et al., 2022). Despite numerous advancements in high-speed alternator designs, existing configurations remain inadequate for aerospace-grade operations because of unresolved thermal and mechanical limitations. Radial flux machines are more suitable than axial flux designs for ultra-high-speed aerospace applications because of their superior rotor balance, shorter thermal paths and better dynamic stability. However, conventional radial flux generators with steel cores and solid copper windings experience severe eddy and thermal losses that degrade their efficiency and reliability. Based on the back electromotive force (EMF) principle, the generator's performance is contingent upon the effective conversion of mechanical energy into electrical energy.

To address these challenges, this study introduces a high-speed (10,000 RPM, 500 Hz) radial flux permanent magnet synchronous generator (RFPMG) utilising advanced Finemet and SMC materials with Litz wire windings. The design and optimisation were conducted using ANSYS Maxwell and Motor-CAD, ensuring compliance with aerospace standards (IEC 60034-1, SAE ARP4990 and IEEE 1812-2014) (Du et al., 2022, 2024; Ismagilov et al., 2021; Liao et al., 2024). The Finemet stator significantly reduces the core loss, whereas the SMC rotor minimises the eddy current effects, thereby enabling a high-frequency and thermally stable operation. Furthermore, Finemet exhibits magnetic stability across a wide frequency and temperature range, and when combined with SMC, it enhances thermal safety and system efficiency by minimising eddy current generation and improving heat dissipation (Chebak et al., 2010; Chen et al., 2024; Jiang et al., 2023; Shao et al., 2021; Talebi et al., 2021; Torun and Swaminathan, 2019; Zhang et al., 2019).

In conclusion, this study details the design and multiphysics simulation of an ultra-high-speed permanent-magnet synchronous generator (PMSG), which incorporates Finemet as the stator material and SMC as the rotor material, complemented by Litz wire windings to minimise AC losses. The proposed Finemet–SMC configuration ensures exceptional electromagnetic efficiency, effective thermal management and high mechanical reliability at an operational speed of 10,000 RPM. These innovations lay a robust foundation for the development of the next generation of lightweight, high-efficiency and thermally stable synchronous aerospace generators, aligning directly with the global shift towards hybrid and fully electrified aircraft propulsion platforms.

## 2. Current Trends and Identified Challenges

Research on high-speed PMSGs has progressed significantly in response to the increasing demand for MEA and hybrid propulsion systems. These generators are valued for their compactness, high efficiency and reduced weight, although challenges persist in managing core loss, temperature rise and mechanical stress. Ismagilov et al. (2020) demonstrated that the use of amorphous alloy cores can reduce core loss by five to seven times and decrease system mass. Gan et al. (2024) further enhanced efficiency by employing Litz wire windings, which lower AC loss and improve electromagnetic control. Taha et al. (2023) and Pasquinelli et al. (2021) emphasised that radial flux configurations provide superior rotor stability for high-speed aerospace applications, whereas Vavilov et al. (2019) and van der Geest et al. (2015) validated high-speed prototypes through simulations and testing. Advanced magnetic materials have been pivotal in enhancing the performance and reducing the weight of these devices. Studies utilising Finemet, amorphous alloys and SMC (Fernando et al., 2017; Ismagilov et al., 2020; Qu et al., 2023;; Vijayakumar et al., 2008) have achieved significant reductions in eddy current loss and thermal stress. Fernando et al. (2017) found that optimised silicon steel offers lower losses and mass compared to cobalt–iron alloys. Varyukhin et al. (2019) achieved a power-to-mass ratio of 4 kW/kg, demonstrating the effectiveness of lightweight magnetic cores in aerospace applications. Thermal management is essential for ensuring system reliability. (Hu et al., 2023; Liu et al., 2011) and (Hu et al., 2023) highlighted that amorphous materials mitigate temperature rise and cooling demand. The multi-field coupling and finite element models developed by Xing et al. (2017) and Feng et al. (2024) demonstrated improved accuracy in predicting the loss distribution and heat transfer, which is critical for weight-sensitive aerospace environments. Reliability-oriented and multi-phase design have significantly enhanced efficiency (>93%), fault tolerance and power-to-weight ratio, thereby meeting aviation safety

standards such as MIL-STD-704F. In parallel, Ning et al. (2012) examined hybrid excitation structures to facilitate flexible voltage regulation and achieve compact designs.

Despite the extensive research on high-speed aerospace generators, most previous studies have focussed on the electromagnetic, thermal or mechanical performance in isolation, lacking a comprehensive multiphysics analysis. The use of amorphous and nanocrystalline materials has been limited to partial tests rather than complete generator systems. Additionally, the combined effects of Finemet and SMC on efficiency, weight and thermal behaviour have not been thoroughly investigated. Few studies have included techno-economic or reliability assessments, resulting in gaps in understanding real-world feasibility under aerospace standards, such as IEEE 1812-2014, IEC 60034-1 and SAE ARP4990. This study presents a Finemet–SMC-based radial flux generator with an integrated electromagnetic–thermal–mechanical design framework optimised for operation at 10,000 RPM. The proposed system achieves notable reductions in loss, temperature and weight, supported by a detailed techno-economic comparison with conventional designs, representing a novel contribution to lightweight, high-efficiency aerospace generators.

### 3. Methodology

#### 3.1 Electromagnetic topology and structural layout

The proposed design shown in Figure 1 represents a radial-flux permanent-magnet synchronous generator (RFPMG). The left panel illustrates the 3-dimensional isometric geometry, while the right panel presents the radial cross-sectional view of the machine. A solid shaft (grey) supports the inner rotor core (cyan/aqua-blue), over which surface-mounted permanent magnets (yellow) are uniformly placed to generate radial magnetic flux across the air gap. Surrounding the rotor, the stator structure (red) forms the main magnetic return path and provides mechanical rigidity. The stator tooth regions (green) guide magnetic flux towards the yoke and contain slot spaces intended for multi-phase armature windings (not shown in the schematic for clarity). This surface-mounted inner-rotor configuration ensures strong flux linkage, reduced eddy losses and high-speed electromagnetic stability. The compact geometry and material layout make the design suitable for next-generation applications, such as aerospace power units, high-density portable power systems and renewable energy conversion platforms (wind, hydrokinetic or micro-turbine-based), where efficiency, lightweight implementation and reliability are critical.

The internal behaviour of the generator under load conditions is depicted by the per-phase equivalent circuit shown in Figure 2. This circuit elucidates the relationship between the generated electromotive force ( $E_{ph}$ ), armature impedance ( $Z_a$ ) and terminal voltage ( $V_t$ ) during operation. The impedance  $Z_a$  comprises armature resistance ( $R_a$ ), which accounts for copper loss and synchronous reactance ( $X_s$ ), representing the combined effects of leakage reactance ( $X_L$ ) and armature reaction ( $X_a$ ). These parameters directly influence voltage regulation, current magnitude and the power angle ( $\delta$ ), all of which govern power transfer capability and steady-state stability. This equivalent circuit forms the analytical foundation for evaluating voltage regulation, load dynamics, power factor and overall efficiency in high-speed aerospace-grade synchronous generators, where compactness, thermal reliability and operational stability are mission-critical.

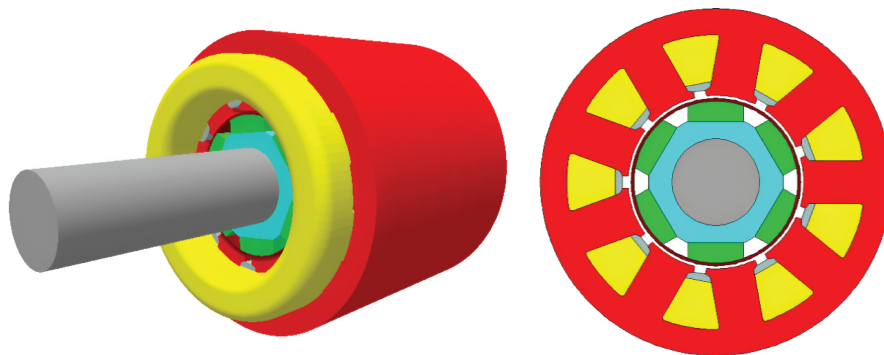


**Figure 1.** 3D and cross-sectional views of a radial flux proposed design generator.

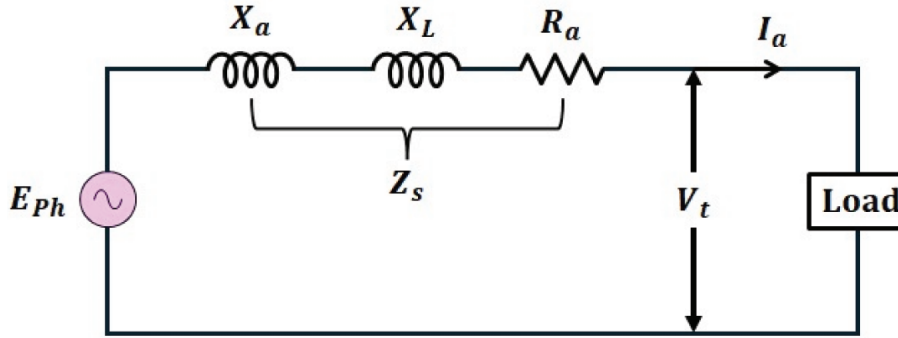


**Figure 2.** Per-phase equivalent circuit of a high-speed radial flux generator.

### 3.2 Geometry design aligned with aerospace standards

Table 1 delineates the principal geometric parameters of the proposed high-speed aerospace generator, which was optimised for compactness, mechanical robustness and electromagnetic performance at 10,000 RPM and 500 Hz. The design incorporates a 6-pole, 9-slot fractional-slot winding configuration, which is recognised for its minimal cogging torque and elevated winding factor, making it particularly suitable for high-speed aerospace applications. The core dimensions, including a 2 mm air gap, 120 mm stator outer diameter, 56 mm rotor outer diameter and 7 mm magnet thickness, were optimised to achieve a balance between efficiency, stability and thermal safety. A 1 mm Inconel 718 rotor band and 30 mm shaft were employed to ensure safe operation under significant centrifugal and torsional stress. The geometry adheres to the IEEE 1812-2014, IEC 60034-1 and SAE ARP4990 standards, which encompass mechanical strength, magnetic loading and thermal margins (IEC60034-1:2022 | IEC, n.d; IEEE SA - IEEE1812-2014, n.d; SAE International | Advancing mobility knowledge and solutions, n.d). The finalised model, developed using ANSYS Motor-CAD, incorporates all design dimensions to facilitate an accurate simulation of electromagnetic losses and temperature increase, thereby ensuring both manufacturability and readiness for aerospace certification.

### 3.3 Electromagnetic and thermal modelling of the generator

To evaluate the behaviour of the proposed high-speed generator under full-load aerospace operating conditions, a combined electromagnetic and thermal model is developed using multiphysics simulation tools. The generator operates at 10,000 RPM and 500 Hz, which introduces challenges such as magnetic saturation, core losses and elevated temperature rise.

The electromagnetic behaviour is governed by Maxwell's equations, particularly Faraday's and Ampere's Laws:

$$\nabla \times E = -\frac{\partial B}{\partial t} \quad (1)$$

$$\nabla \times H = J + \frac{\partial D}{\partial t} \quad (2)$$

To solve these equations in finite element simulation, the magnetic vector potential method is used:

$$B = \nabla \times A, \nabla \times \left( \frac{\nabla}{\mu} \times A \right) = J \quad (3)$$

where non-linear B–H curves of Finemet and SMC materials are used to account for the magnetic saturation and permeability behaviour. The rotor magnets are modelled with defined remanence and coercivity to simulate realistic flux density profiles. Simulation is performed in ANSYS Maxwell, both in 2D and 3D environments.

Copper loss in the stator winding is calculated using:

$$P_{cu} = I^2 R \quad (4)$$

**Table 1.** Key geometric design parameters of the proposed aerospace generator.

Parameter	Value	Unit
Number of stator slots	9	
Number of poles	6	
Stator outer diameter	120	mm
Shaft diameter	30	mm
Airgap length	2	mm
Magnet thickness	7	mm
Banding thickness	1	mm

where R includes the AC resistance due to skin and proximity effects, for which Litz wire is used to reduce eddy losses. Core losses in the stator and rotor are estimated using the generalised Steinmetz equation (Roy et al., 2017):

$$P_{core} = k_h f B^\alpha + k_e f^2 B^2 \quad (5)$$

where  $f$  is frequency,  $B$  is peak flux density and  $k_h$ ,  $k_e$ ,  $\alpha$  are material constants (specific to Finemet and SMC). Magnet losses and additional eddy current losses in rotating surfaces are also captured through time-domain loss calculation in Maxwell. The heat generated due to total losses is applied as input to a thermal model in Motor-CAD. The machine's temperature distribution is simulated using the heat conduction equation (Kazeem Iyanda et al., 2023):

$$\rho c_p \frac{\partial T}{\partial t} = \nabla \cdot (k \nabla T) + Q \quad (6)$$

where  $\rho$  is the material density,  $c_p$  is the specific heat capacity,  $k$  is the thermal conductivity,  $T$  is the temperature distribution inside the corresponding material region (stator core, rotor core, magnet and windings) and  $Q$  represents the volumetric heat source generated by copper loss, core loss and magnet loss. The material-dependent thermal properties used in the simulation include Finemet ( $23 \text{ W/mk}$ ), SMC ( $6 \text{ W/mk}$ ) and copper ( $385 \text{ W/mk}$ ). Appropriate

boundary conditions were applied to model both natural and forced convection, with the ambient temperature set to  $40^\circ\text{C}$  and convective heat transfer imposed on the outer casing and shaft surfaces. The thermal simulation results demonstrated that the temperatures of both the winding and the stator core remained well within their safe operational limits, reaching only  $89^\circ\text{C}$  in the proposed Finemet–SMC design compared to  $142^\circ\text{C}$  in the conventional generator. The magnetic flux-density distribution confirmed linear magnetic behaviour throughout the stator and rotor, with no signs of local saturation. Overall, the Finemet–SMC-based generator exhibited reduced thermal stress, improved cooling effectiveness and significantly enhanced stability under aerospace-rated loading conditions, strengthening its suitability for lightweight, high-speed electric propulsion applications.

### 3.4 Strategic material selection and engineering parameters

Material properties are one of the key parameters in determining the feasibility and performance of electric machines for aerospace applications. The rotor core and stator core of the new generator configuration employ ultra-highly optimised soft magnetic materials. They possess high electrical resistivity with extremely thin lamination thicknesses, which significantly reduce the eddy current losses under high-frequency operation. This is especially required in UHGs where reduction of loss means system efficiency and thermal stability enhancement directly. Table 2 also show that the new materials have relatively high yield stress and low Young's modulus but are structurally strong enough to resist excessive centrifugal forces at flight and mechanically flexible. Lower densities in the new design are directly translated to mass savings a highly desirable advantage for aerospace applications requiring higher power-to-weight ratios. Table 2 also shows that the traditional design, as high as its Young's modulus and density, is disadvantageously lower in electrical resistivity and has more laminations, which correspond to higher iron losses. As it is currently, it is less effective and less suitable for small, lightweight and low-power applications. Among various soft magnetic materials, Hiperc 50 is chosen as the baseline reference due to its extensive use

**Table 2.** Material properties of the proposed and conventional aerospace generator designs (Tian et al., 2025; Wang and Wang, 2011).

Parameters	Proposed design material		Conventional design material	Unit
	Stator core	Rotor core		
Lamination thickness	0.018	0.05 mm	0.15	mm
Relative permeability ( $\mu_r$ )	80,000–100,000	200–500	18,000	
Poisson's ratio	0.3	0.32	0.3	
Thermal conductivity	23	6	14.5	W/m/K
Specific heat capacity ( $C_p$ )	480	500	460	J/kg/K
Young's coefficient	140,000	160,000	207,000	Mpa
Curie temperature	570	560	980	°C
Yield stress	800	200	393	Mpa
Density	7,300	7,500	8,110	kg/m <sup>3</sup>
Electrical resistivity	1.2E–6	20E–6	4.06E–7	$\Omega/m$

in high-speed aerospace machines. By enabling lower losses, lower weight and improved thermal management, the material configuration described here assures improved overall system performance, reliability and energy efficiency under harsh aerospace environments.

### 3.5 Simulation workflow

The comprehensive simulation workflow depicted in Figure 3 delineates the entire design and analysis procedure for the proposed aerospace generator. This workflow methodically integrates the electromagnetic and thermal domains through a sequential approach, commencing with the definition of the application requirements and culminating in the final performance evaluation. The process encompasses topology selection, material assignment, boundary condition configuration, finite element simulation using ANSYS Motor-CAD, thermal modelling and integration of multiphysics data. This systematic methodology ensures precise performance prediction and establishes the Finemet–SMC-based generator as a dependable and high-efficiency solution for aerospace applications.

## 4. Simulation Results and Comparative Performance Evaluation

### 4.1 Terminal voltage evaluation of proposed and conventional aerospace generators

Figure 4 compares the terminal voltage waveforms for both generator designs in aerospace. Figure 4(a) presents the terminal voltages for the new generator design in aerospace, while Figure 4(b) presents the same in voltage amplitude consistency and waveform symmetry. In Figure 5(a), the amplitude of the peak terminal voltages between phases is approximately  $\pm 430$  V (Ph1–Ph2, Ph2–Ph3 and Ph3–Ph1). Figure 4(b) illustrates that the identical voltages reach an amplitude of merely  $\pm 330$  V. The higher voltage amplitude of the proposed design would denote better electromagnetic flux linkage and better optimisation of coil configuration, likely due to the Litz wire windings and magnetic circuit improvement. Furthermore, Figure 4(a) waveform is also more sinusoidal and symmetrical, indicative of a balanced phase output necessary to minimise harmonics and ensure smooth torque production in aerospace applications. Figure 4(b), by comparison, is somewhat more distorted in waveform and less symmetrical, potentially implying less efficiency and greater thermal losses at increased speeds. The improved waveform quality and higher voltage rating of the new generator demonstrate its potential for use in high-reliability, high-efficiency aerospace power systems, especially where space and weight constraints demand optimum performance from miniature electrical machines.

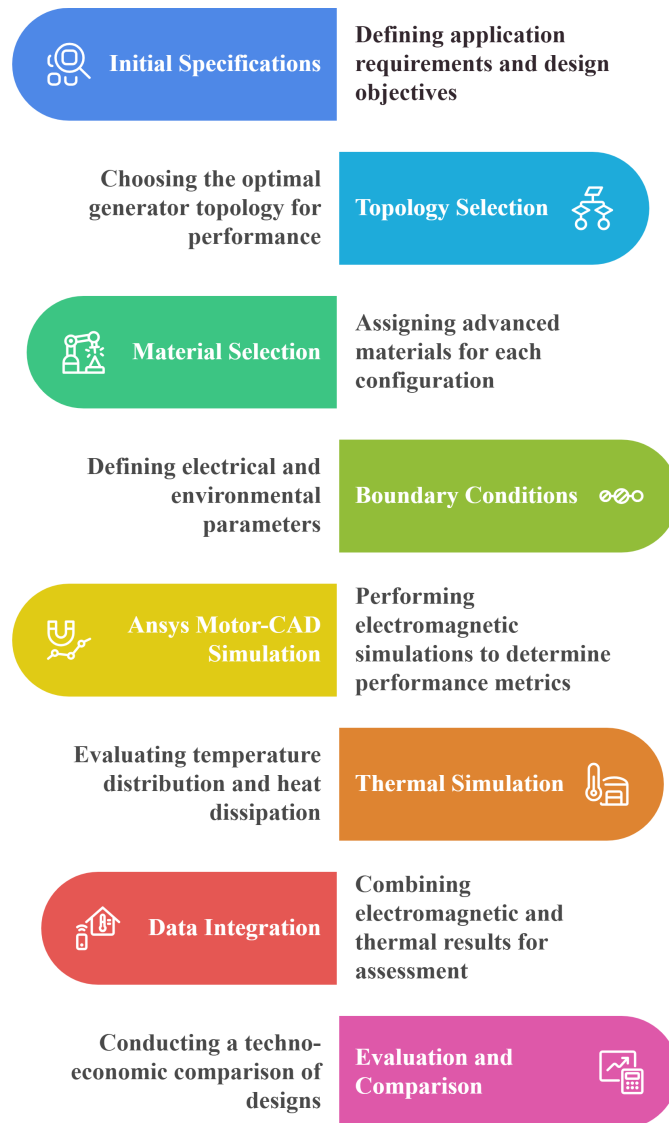


**Figure 3.** Simulation workflow for performance evaluation of proposed and conventional aerospace generators.

## 4.2 Torque envelope and speed characteristics of the generator

Figure 5(a) presents the torque–rotational speed characteristics of the proposed Finemet–SMC-based synchronous generator. Although the rated operating speed is 10,000 rpm, the simulation is extended to higher rotational speeds to evaluate over-speed tolerance, torque stability and field-weakening behaviour – critical performance indicators for aerospace power applications. The design maintains an almost constant torque across the nominal operating region for all applied advance angles. Beyond approximately 17,000–18,000 rpm, the machine transitions into the field-weakening region, where torque gradually decreases. Notably, the torque envelope remains stable beyond 30,000 rpm, demonstrating that the Finemet–SMC combination significantly reduces iron losses and enables reliable high-speed operation with an extended constant-power range. Figure 5(b) illustrates the torque–rotational speed response of the conventional Hyperco-50-based generator. While torque remains nearly constant at low speeds, field-weakening begins earlier at  $\approx 15,000$ – $16,000$  rpm, and torque declines sharply with increasing speed. The reduced high-speed capability is attributed to the higher hysteresis and eddy-current losses of Hyperco-50, which limit magnetic performance at elevated frequencies. Overall, the comparison confirms that the proposed

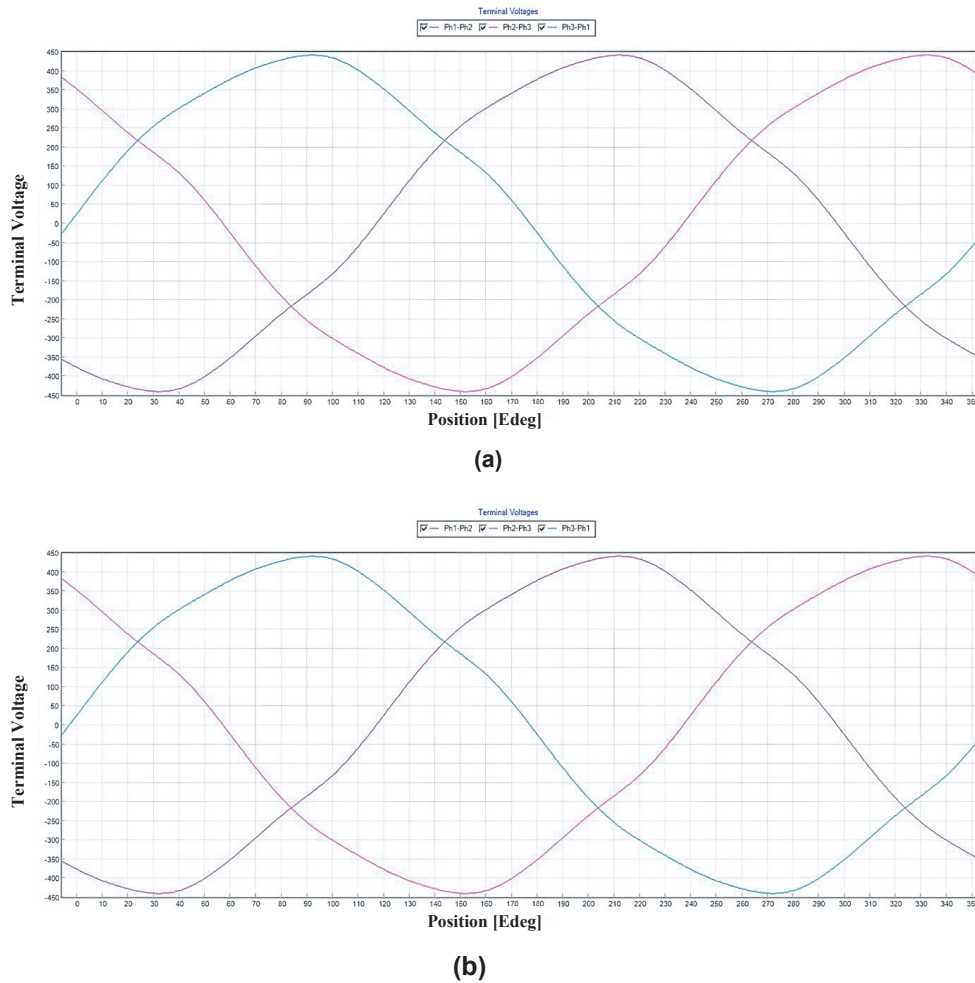


**Figure 4.** Phase-to-phase terminal voltages: (a) proposed Finemet-SMC-based generator and (b) Hiperco 50-based conventional generator. SMC, soft magnetic composites.

Finemet-SMC generator exhibits superior high-speed characteristics, delayed field-weakening onset, enhanced torque sustainability and a significantly wider effective operating bandwidth than the conventional machine.

### 4.3 Power-speed characteristics and high-speed capability analysis

Figure 6(a) and Figure 6(b) depict that the power-speed characteristics of the proposed Finemet-SMC generator and the conventional Hiperco 50-based design, respectively, evaluated across various current advance angles. A distinct performance difference is evident between the two machines throughout the entire operating range. In Figure 6, the proposed generator demonstrates a significantly higher power extraction capability from low to high speeds. The consistently steeper power gradient is attributed to the superior electromagnetic loading facilitated by the Finemet stator and the high-resistivity SMC rotor. These materials effectively minimise leakage flux, reduce high-frequency losses and enhance the effective air-gap flux density. As a result, the power envelope remains higher for all advance angles ( $120^{\circ}$ – $180^{\circ}$ ), indicating strong suitability for high-speed aerospace operations. Conversely, Figure 6(b) reveals that the conventional Hiperco 50-based generator experiences a more rapid decline in power as rotational speed increases. The earlier collapse of the power envelope is primarily due to higher eddy-current loss and increased magnetic drag in the laminated steel core, which limits sustained power delivery above approximately 20,000–24,000 rpm. A direct comparison of the two envelopes shows that the proposed machine delivers 20–35% more usable power in the mid-speed range (10,000–18,000 rpm) and maintains a substantially broader and more stable high-speed operating band beyond 20,000 rpm. This advantage confirms that the Finemet-SMC

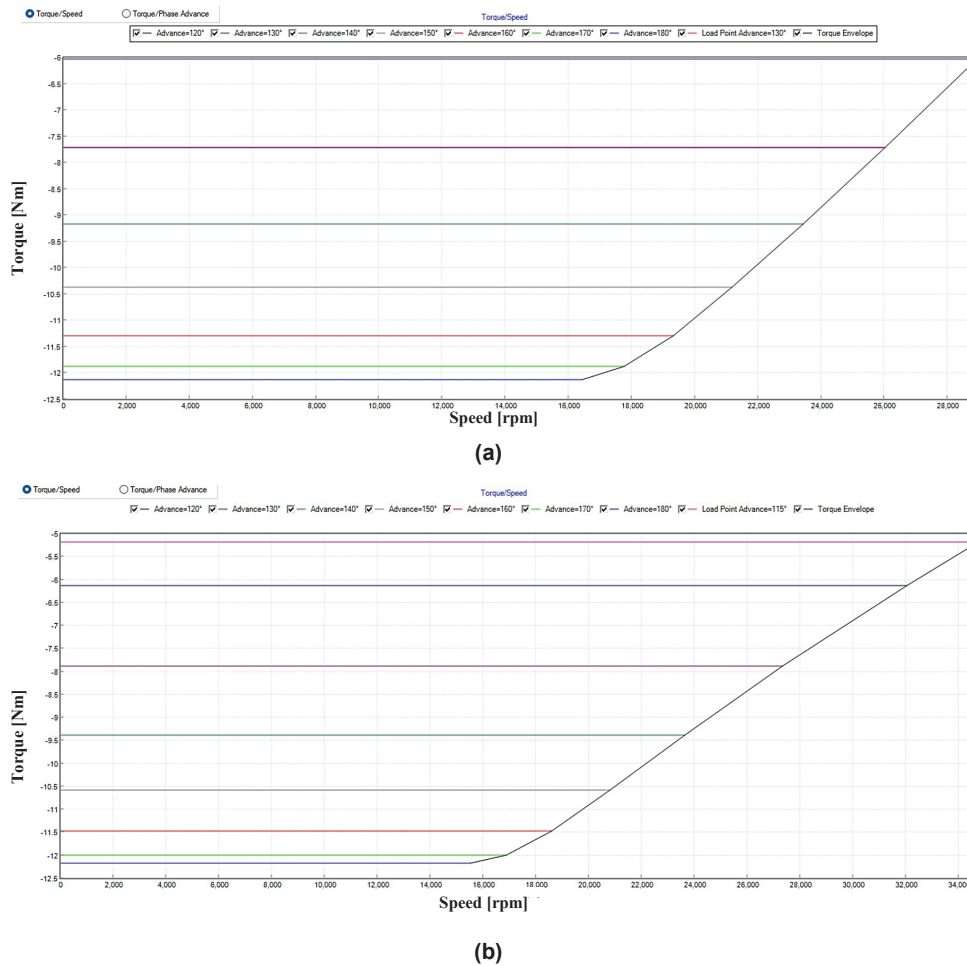


**Figure 5.** Torque–speed characteristics of: (a) proposed Finemet–SMC-based generator and (b) Hiperco 50-based conventional generator. SMC, soft magnetic composites.

configuration enhances torque production, minimises loss-induced derating and ensures stable output for high-speed aerospace propulsion systems. Although the generator is nominally rated at 10,000 rpm, the power–speed curves are extended up to 30,000 rpm to assess the overspeed capability margin required in aerospace platforms. Short-duration overspeed events can occur during rapid throttle commands, emergency power demands, or regenerative braking sequences in hybrid-electric propulsion architectures. Certification guidelines – such as IEC 60034-1 and SAE ARP4990 – recommend validating performance at 200%–300% of the nominal speed to ensure mechanical and electromagnetic robustness under such transient conditions. The proposed Finemet–SMC generator maintains stable behaviour across this extended speed range, confirming that it possesses adequate safety margins and can withstand the aerodynamic, thermal and structural stresses encountered in modern high-speed aviation environments.

#### 4.4 Flux density distribution analysis

Figure 7(a) and Figure 7(b) show the magnetic flux density distribution of the new and conventional generator designs, respectively, operating under similar working conditions. In the new structure, in which Finemet is employed in the stator and SMC in the rotor, the flux density is at a maximum of approximately 1.48 T with even and symmetric flux lines along the rotor–stator interface. The colour map is utilised to indicate the flux density magnitude, with blue signifying the low flux regions ( $\sim 0$  T) and red being the high flux regions approaching saturation ( $\geq 1.5$  T). Most of the magnetic path in Figure 7(a) is within the green to light yellow region ( $\sim 0.7$ – $1.4$  T), indicating that the magnetic circuit is well within the linear region of the core materials. This ensures lower core losses and a higher overall efficiency.

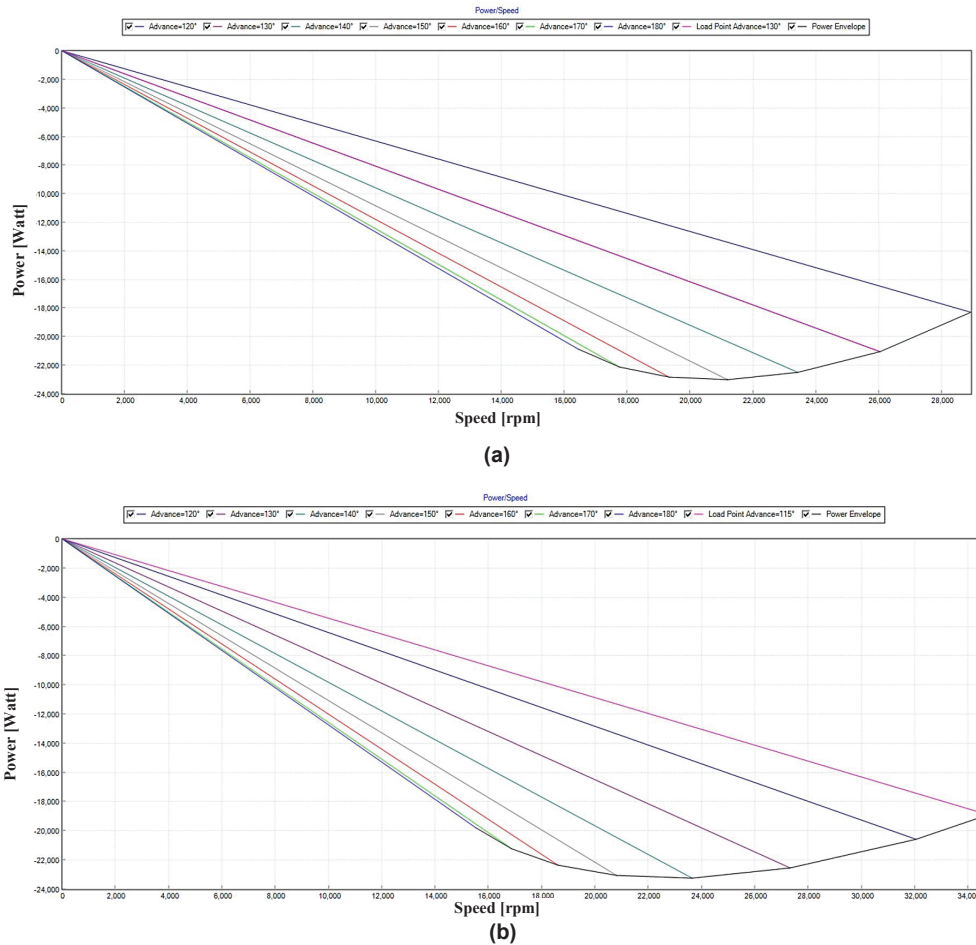
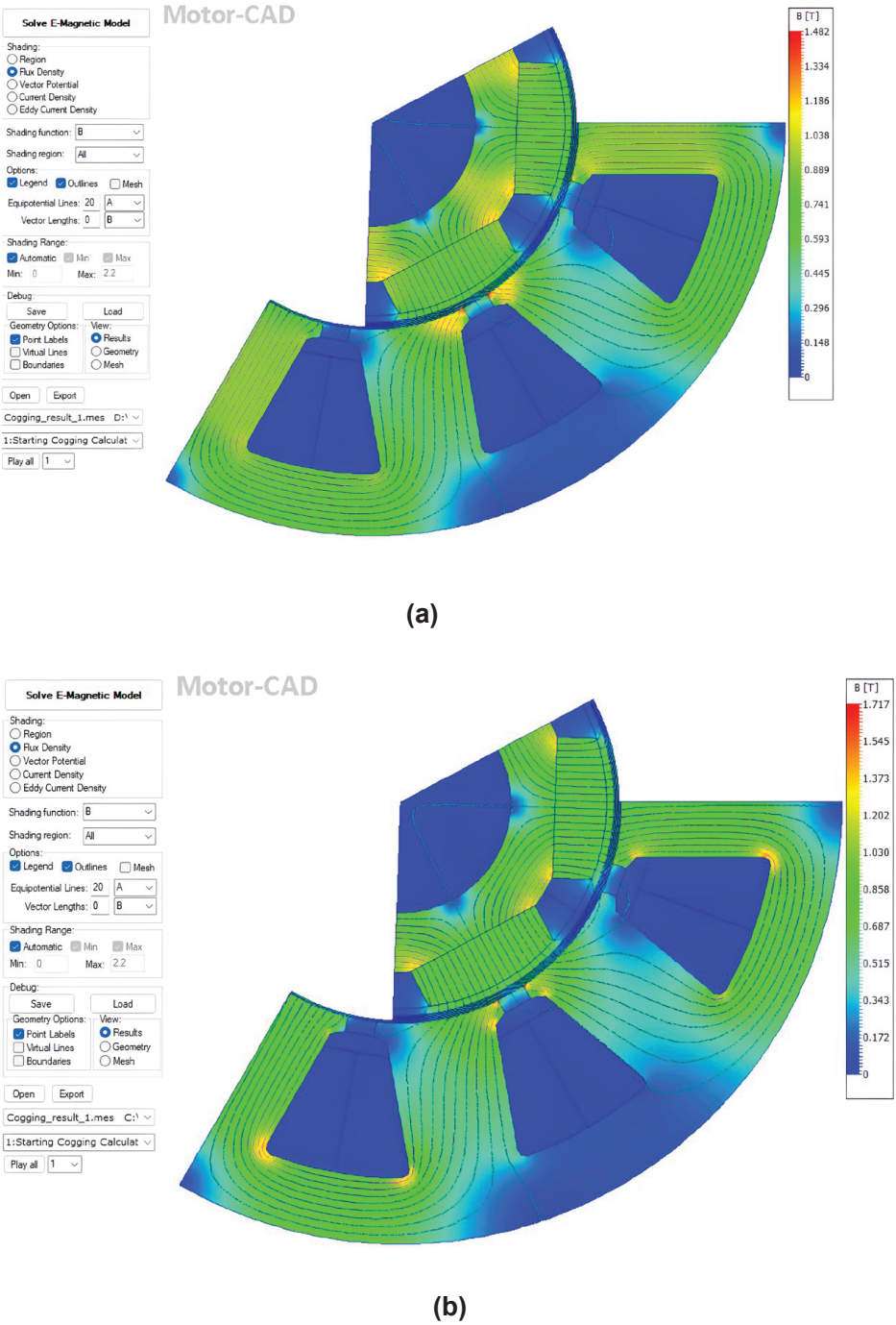


**Figure 6.** Power–speed envelopes of (a) the proposed Finemet–SMC-based generator and (b) the conventional Hiperco 50 generator. SMC, soft magnetic composites.

On the contrary, the conventional design in Figure 7(b), with a based on high-performance cobalt–iron alloy core material (Hiperco 50), possesses a maximum flux density of approximately 1.7 T that is illustrated by orange to red regions concentrated at the stator teeth tips and yoke corners. They are prone to higher hysteresis and eddy current losses, especially at high frequency operation. Besides that, flux lines in the classical model appear denser and slightly more rounded in high-density areas, reflecting less efficient magnetic utilisation and greater local thermal stress. This comparative flux visualisation emphasises the benefit of using Finemet and SMC in the design at hand to suppress saturation effects, maintain magnetic linearity and assure high-efficiency operation under aerospace-grade conditions.

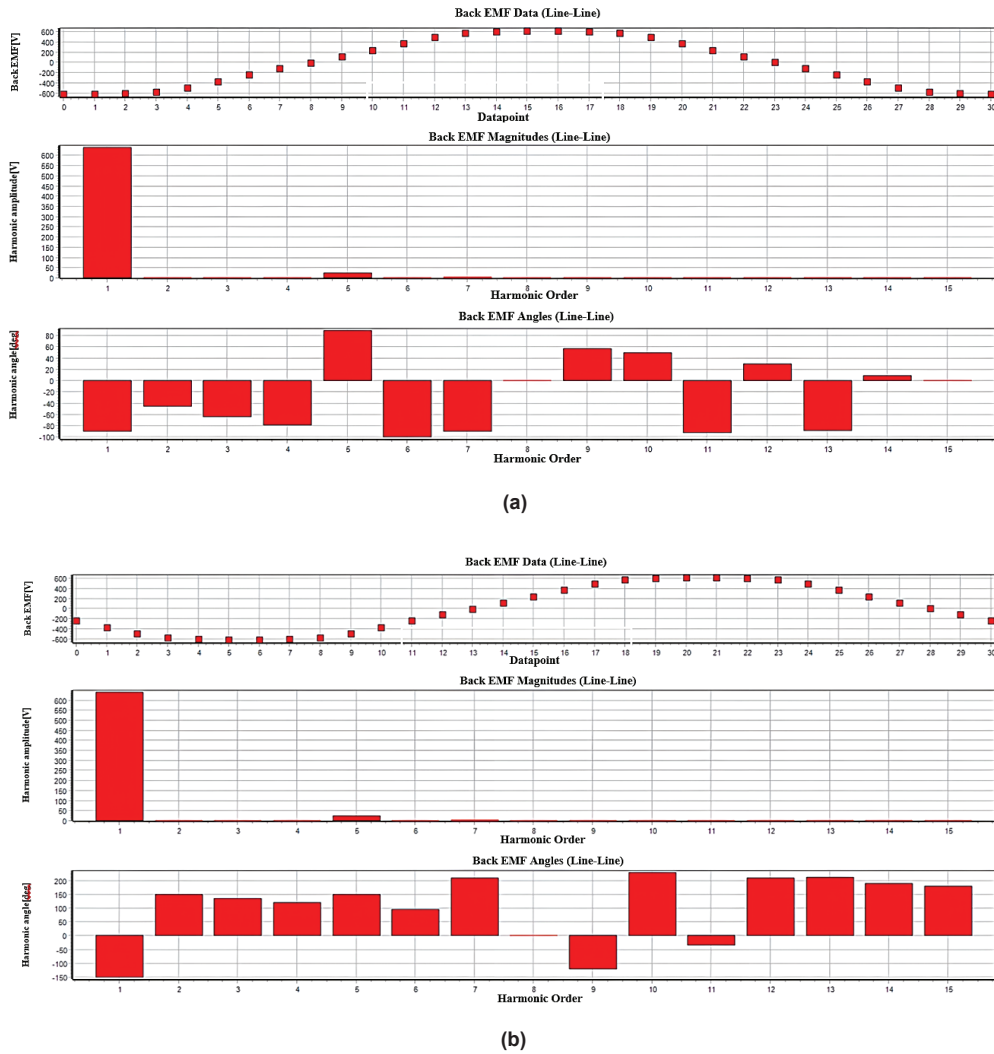
#### 4.5 Back EMF characterisation and harmonic performance assessment

Figure 8(a) and Figure 8(b) present, respectively, the comparative Back EMF waveforms and harmonic content of the proposed Finemet–SMC generator and the conventional Hiperco 50-based generator based on Ansys Motor-CAD simulation. All three, line-to-line Back EMF waveform, harmonic amplitude spectrum and harmonic phase angles, are presented in each figure. In the specified generator of Figure 8(a), the waveform is highly sinusoidal and symmetrical with peak voltages of approximately  $\pm 600$  V. There is a prominent fundamental component with small higher-order harmonics in the harmonic spectrum, which confirms reduced waveform distortion. The trend is a reflection of improved magnetic circuit and efficient winding design, which find their implementation in lower torque ripple and improved electromagnetic performance. On the contrary, Figure 8(b) shows that the conventional design generates a little smaller peak Back EMF of about  $\pm 530$  V and also shows prominent 5th and other harmonic orders. These harmonics place higher electromagnetic stress and presumably higher



**Figure 7.** Comparison of magnetic flux density distribution: (a) proposed Finemet-SMC-based generator and (b) Hiperco 50-based conventional generator. SMC, soft magnetic composites.

torque ripple under working conditions. Moreover, the phase angle spread is less uniform in the conventional configuration, indicating less predictable phase behaviour under dynamic conditions. Overall, the new design embodies improved waveform quality, improved harmonic suppression and more fundamental voltage output, ideal for aerospace uses where performance, reliability and thermal efficiency are key.



**Figure 8.** Back EMF and harmonic signature analysis: (a) proposed Finemet-SMC-based generator and (b) Hiperco 50-based conventional generator. SMC, soft magnetic composites.

#### 4.6 Harmonic characterisation of electromagnetic torque

Figure 9 illustrates the harmonic analysis of both generator designs, as evaluated using ANSYS Motor-CAD. The Finemet-SMC generator (Figure 9[a]) exhibited a smoother torque profile with a reduced fluctuation amplitude compared to the Hiperco 50 model (Figure 9[b]). The Fast Fourier Transform (FFT) results corroborate that the proposed design significantly diminishes the 6th and 9th harmonic components, thereby minimising torque ripple and electromagnetic noise. Despite both designs having similar phase distributions, the reduced harmonic magnitudes in the Finemet-SMC generator suggest a more symmetrical magnetic field and decreased vibration. Overall, the Finemet-SMC design demonstrated that superior harmonic suppression, reduced cogging torque and smoother electromagnetic torque attributed to Finemet's high permeability and low core loss, as well as SMC's low eddy current losses, rendering it particularly suitable for high-speed aerospace applications.

#### 4.7 Thermal stability comparison of proposed and conventional aerospace generators

Thermal performance comparison in Table 3 reveals the spectacular superiority of the new generator design over the conventional Hiperco 50-based solution. The new Finemet + SMC design is spectacularly lowering overall thermal losses (637.4 W to 165.4 W) through new core materials and Litz wire windings. Significantly, the stator iron loss is going down spectacularly from 226.6 W to a mere 0.6027 W, reflecting magnetic efficiency improvement.

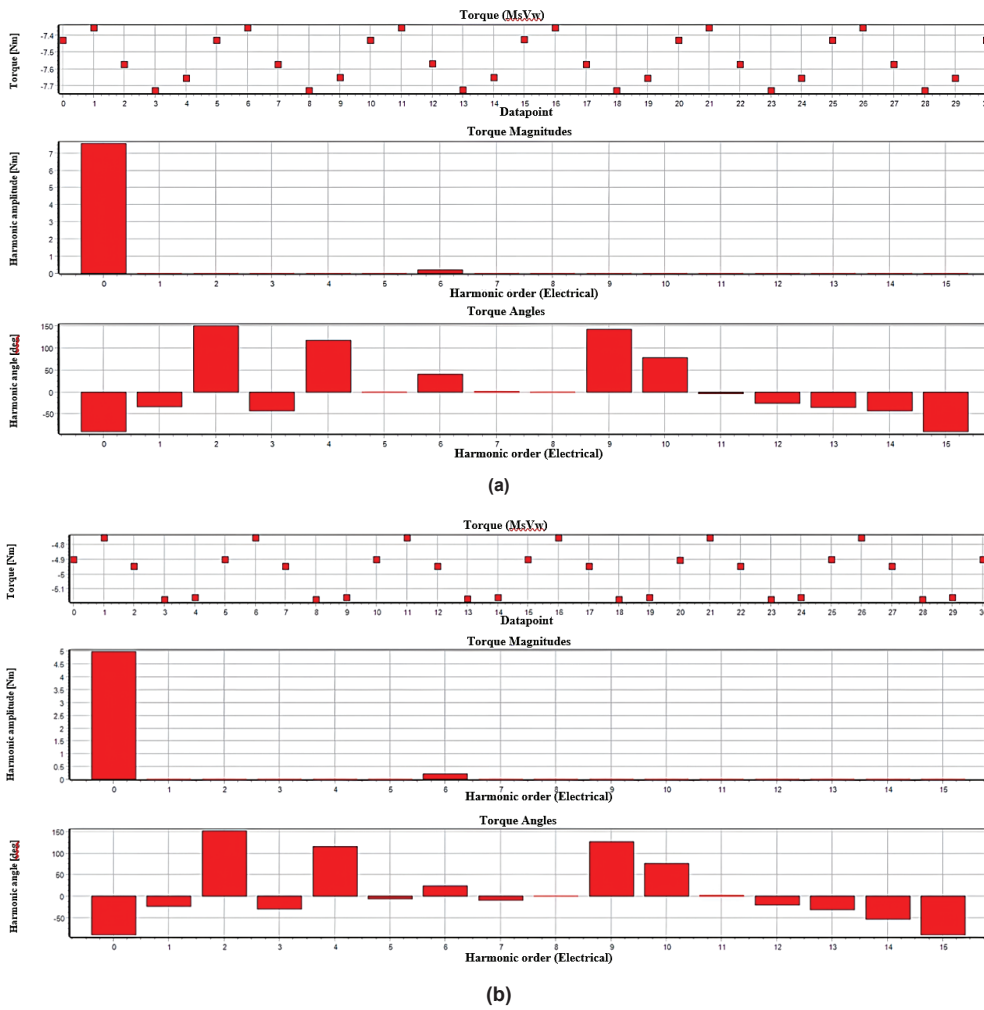


**Figure 9.** Torque waveform and FFT analysis: (a) proposed Finemet-SMC-based generator and (b) Hiperco 50-based conventional generator. FFT, fast Fourier transform; SMC, soft magnetic composites.

In addition, the maximum temperatures of the curving, stator and rotor are diminished significantly in the new design, enhancing operating safety and component longevity. The margin of thermal limit is expanded from 15% to 42% and that gives a larger margin of ruggedness against thermal cycling typical of aerospace operating conditions. As may be seen from Table 3, the passive convection reference system is replaced by a forced-air technique utilising aluminium fins and ducting. The novel thermal management not only maintains system temperatures well below critical values, but it also enables long-term sustainable operation in extreme aerospace conditions.

Thermal Rise Estimation Based on Losses.

We use the basic thermal equation (Hamila et al., 2017):

$$\Delta T = P_{\text{loss}} \times \theta$$

where  $\Delta T$  is the temperature rise in  $^{\circ}\text{C}$ ,  $P_{\text{loss}}$  is the total thermal loss in W, and  $\theta$  is the thermal resistance ( $^{\circ}\text{C}/\text{W}$ ), typically  $0.3^{\circ}\text{C}/\text{W}$  for compact aerospace machines.

The thermal performance comparison highlights a substantial enhancement in the proposed design. The conventional generator exhibited a total power loss of 737 W, resulting in a temperature increase of  $221.1^{\circ}\text{C}$  at a thermal resistance of  $0.3^{\circ}\text{C}/\text{W}$ . Conversely, the proposed design reduces the power loss to 296.4 W, thereby limiting the temperature rise to  $88.9^{\circ}\text{C}$  – a reduction of  $132.2^{\circ}\text{C}$ . This marked decrease in the operating temperature improves the thermal stability, extends the insulation life and enhances the overall system reliability, thereby affirming the superior thermal management capabilities of the proposed generator for high-power aerospace applications.

**Table 3.** Comparative thermal parameters and cooling techniques of conventional and proposed aerospace generators

Thermal parameter	Conventional aerospace generators	Proposed aerospace generators	Unit
Winding loss	450.7	232.5	(W)
Iron loss – stator core	226.6	0.6027	(W)
Iron loss – rotor core	0.3087	0.02588	(W)
Magnet loss	29.53	33.82	(W)
Additional loss	29.83	29.42	(W)
Total loss	737	296.4	(W)
Total thermal loss	637.4	165.4	(W)
Max winding temperature	142	89	(°C)
Max stator temperature	168.4	92.5	(°C)
Max rotor temperature	157.9	88.1	(°C)
Thermal limit margin	15	42	%
Thermal conductivity of core	14.5	23	
Cooling mechanism	Passive convection	Directed forced air	

## 5. Discussion

In the multiphysics simulation results shown here reveal that the proposed Finemet–SMC-based radial-flux PMSG exhibits significant performance improvements over its conventional Hiperco 50-based counterpart under identical operating conditions. Various features of the comparison presented in Figure 10 consistently demonstrate enhanced electromagnetic, thermal and mechanical behaviours, all of which are very important for high-speed aerospace electrical machines. Electromagnetically, the proposed generator shows greatly increased output power and efficiency. For instance, the output power is increased by about 59% (7485.3 W vs. 4711.8 W) while the overall efficiency is increased by 11.2% to become 96.19%. These are clearly related to the distinct magnetic and electrical properties of the materials used. Finemet presents very low hysteresis and eddy-current losses when subjected to high electrical frequency, thereby allowing for higher magnetic loading without core overheating. Meanwhile, the high electrical resistivity of the SMC rotor material has significantly reduced rotor eddy-current loss, which becomes important in high rotational speed conditions. The use of Litz-wire armature windings further reduces AC copper loss due to the reduction in skin and proximity effects at a frequency of 500 Hz. In this respect, the proposed generator is able to produce higher fundamental back-electromotive force (approximately  $\pm 600$  V as opposed to the approximately  $\pm 530$  V for the conventional machine), improved air-gap flux density and superior real power extraction capability. The torque performance also indicates marked improvement. The average electromagnetic torque increases by about 49%, while the torque ripple decreases by 44% relative to that of the Hiperco 50-based generator. Reduced torque ripple leads to smoother mechanical operation, reduced vibration levels and lower acoustic noise – characteristics that are particularly valuable in aerospace applications because of implications for mechanical reliability and rotational stability. Furthermore, an extended torque envelope and delayed onset of field weakening at high rotational speeds suggest greater electromagnetic stability and increased range of constant-power operation for the proposed design. The excellence of the Finemet–SMC configuration is further confirmed by thermal analysis. In particular, the maximum winding temperature reduces by approximately 37%, and the stator temperature decreases by 45%, ensuring that all critical components remain well below the 120°C thermal limit commonly recommended for aerospace electrical machines. This thermal improvement could be essentially attributed to the joint action of reduced electromagnetic losses and the implementation of directed forced-air cooling that is significantly superior compared with passive natural convection. This eventually leads to the nearly 60% reduction of the total on-load loss, improving energy utilisation in addition to enhanced thermal reliability and longer expected service life. Another positive effect consists in the 15.8% improvement of power factor, ensuring enhanced voltage stability and reduced reactive power flow within the system. Structural simulations were also performed as a means of ensuring mechanical robustness for safe operation at high speed. The peak Von-Mises stress in the rotor stays well within the 200 MPa yield strength of the SMC material, even at rotation speed levels up to 10,000 rpm. These facts reveal that the rotor structure does not incur unduly high mechanical deformation due to centrifugal

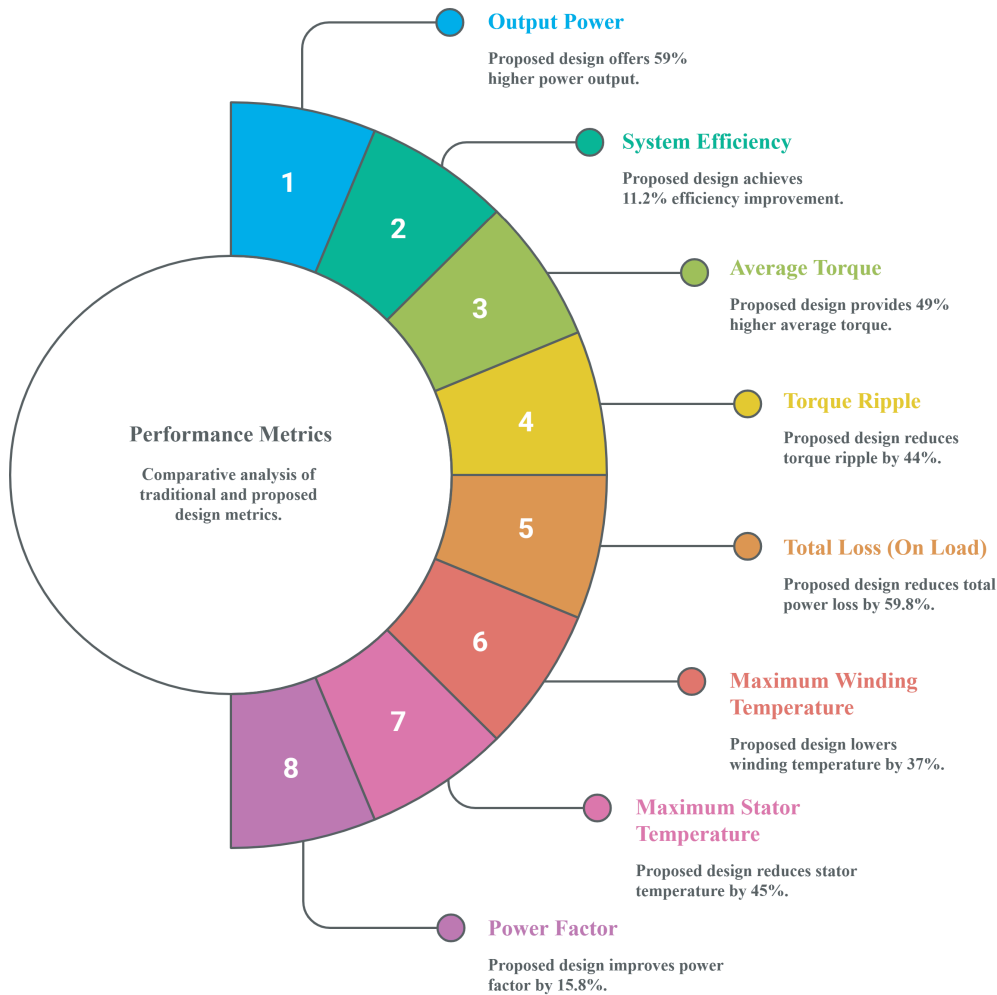


**Figure 10.** Key performance improvements in the proposed Finemet–SMC design. SMC, soft magnetic composites.

loading. The close match among electromagnetic, thermal and mechanical constraints indicates that the proposed generator design is well optimised for aerospace-grade operating conditions.

A particularly noteworthy result of these simulations is the strong prediction for stator iron loss reduction, arising from the ultra-low-loss nature of Finemet and the deployment of ultra-thin laminations of 0.018 mm thickness. Eddy-current losses decrease strongly with reducing lamination thickness, while Finemet's nanocrystalline structure minimises hysteresis losses under high-frequency excitation. However, it has to be pointed out that these results are based on simulation and presume ideal lamination stacking, insulation quality and material properties based on data supplied by the manufacturer. Therefore, the absolute magnitude of the predicted loss reduction should be considered with appropriate caution. From a practical point of view, the manufacturability of ultra-thin Finemet laminations is an important consideration. Commercially, Finemet is produced primarily in rapidly quenched nanocrystalline ribbons, with typical thicknesses in the range of 10–30  $\mu\text{m}$ , consistent with the assumptions here. These ribbons are mechanically fragile and generally not compatible with the conventional punching and stacking processes used for electrical steels. Alternative routes to fabrication may be necessary in practice, such as ribbon winding with impregnation, adhesive stacking with thin insulation coatings, or laser-assisted cutting methods that are optimised to avoid thermal degradation. Experimental prototyping and manufacturing trials are therefore crucial in order to verify the simulated performance and also to quantify any additional losses introduced during fabrication. Overall, the results suggest that the proposed Finemet–SMC-based generator meets all key performance criteria for high-speed aerospace electrical machines in terms of high efficiency, low torque ripple, acceptable thermal margins and mechanical safety. By integrating Finemet's

nanocrystalline magnetic properties with the low-loss and structurally robust characteristics of SMC materials, the proposed design offers a promising pathway towards compact, lightweight and high-efficiency generators for next-generation electrified and hybrid aerospace propulsion systems.

## 6. Comprehensive Techno-Economic Analysis and Industrial Justification

### 6.1 Comparative cost and material analysis of conventional and proposed aerospace generators

Table 4 tabulates the detailed comparative review of material content, weight distribution and cost breakdown of the traditional aerospace generator against the suggested high-speed generator design. The traditional arrangement extensively employs Hiperco 50 in the stator back as well as tooth laminations, contributing mainly to its weight and heavy manufacturing cost. In turn, the new design replaces Hiperco 50 with Finemet FT-3M, which possesses superior magnetic performance and facilitates extreme reductions in component cost and weight. The rotor core, usually composed of Hiperco 50, is replaced by Soft Magnetic Composite (SMC HB1), possessing higher thermal insulation and lower eddy current loss. The armature winding method is also improved via replacement of regular copper with Litz wire, which minimises AC losses at high frequency (500 Hz) and serves to minimise weight as well. Crucially, the total estimated cost of the new design is \$2,159.61, compared to \$4,601.67 for the standard setup, which represents a 53.1% decrease in capital expenditure. This cost-effectiveness, coupled with minimum architecture and material integration with high performance, emphasises commercial and technological viability of the proposed generator for use in future aero-sciences.

### 6.2 Loss breakdown and yearly energy savings

The thermal and electrical efficiency of any aerospace generator is directly proportional to its internal power losses. Based on a comparison between the two, the conventional aerospace generator with Hiperco 50 has a total power loss of 737 W, whereas the new high-speed generator with a Finemet stator, SMC rotor, and Litz wire windings has a significantly lower total loss of 296.4 W.

The difference in loss,

$$\begin{aligned}\Delta P_{\text{loss}} &= 737 - 296.4 \\ &= 440.6 \text{ W}\end{aligned}$$

constitutes a 59.8% reduction in overall losses.

Taking a normal operation time of 4,000 h/year, which is common for aerospace auxiliary or continuous electrical systems, the equivalent yearly energy savings can be determined as:

**Table 4.** Comparative cost and material analysis of conventional vs. proposed aerospace generator designs (Innovation. Carpenter Technology, n.d.; Metal powders | Höganäs, n.d.; VAC - Advanced Magnetic Solutions | VAC, n.d.).

Component	Material (Trad./Prop.)	Weight (kg) (Conv./Prop.)	Cost of conventional aerospace generator (USD)	Cost of proposed design aerospace generator (USD)
Stator lamination (Back)	Hiperco 50/Finemet FT3M	2.469/2.222	1,728.30	666.60
Stator lamination (tooth)	Hiperco 50/Finemet FT3M	2.293/2.064	1,605.10	619.20
Rotor lamination (total)	Hiperco 50/SMC HB1	0.6339/0.5862	443.73	70.34
Armature winding (active)	Copper/Litz wire	2.163/1.114	35.77	33.42
Armature end winding (total)	Copper/Litz wire	2.121/0.546	35.10	16.38
Magnet	Recoma 28	0.6147	737.64	737.64
Rotor banding	Inconel 718	0.1397	11.18	11.18
Shaft (total)	Steel (general)	2.425	4.85	4.85
Total estimated cost			\$4,601.67	\$2,159.61
Cost reduction	53.1%			

$$\begin{aligned} E_{\text{saved per year}} &= 440.6 \text{ W} \times 4000 \text{ h} \\ &= 1762.4 \text{ kWh/year} \end{aligned}$$

Such energy saving reduces the load on the onboard power system, along with reduced cooling requirements, longer component life and system reliability overall. From an ecological perspective as well as a monetary one, such a saving can translate to less fuel consumption on generator-powered aircraft, making operations environmentally friendly as well as cost-effective in the long term.

### 6.3 Long-term energy cost savings and lifecycle impact

Due to the severe operating conditions in aerospace environments, such as frequent thermal cycling, mechanical vibrations and regular maintenance, an optimal service life of 15 years is generally assumed for onboard electrical generators. Based on the calculated annual energy savings of 1,762.4 kWh/year and a conservative global average electricity price of \$0.12 per kWh, annual operating cost savings can be estimated as:

$$E_{\text{saved per year}} \times 0.12 = \$211.488 / \text{year}$$

Total Lifetime Energy Cost Savings:

$$\text{Annual Energy Cost Savings} \times 15 = \$3,172.32$$

These significant lifecycle cost savings of over \$3100 highlights the economic benefits of employing the planned generator architecture. For defence and commercial aviation applications, where operating efficiency and cost of ownership are both major considerations, such long-term energy savings can play a large part in reduced fuel consumption, lower emissions and enhanced return on investment. Additionally, the reduced thermal and electrical stress on system elements lowers maintenance schedules and enhances reliability, substantiating its value in mission-critical aerospace operations.

## 7. Future Research Directions and Development Roadmap

The results shown in this paper represent the outcome of extensive multiphysics simulations that give an insight into the trends of relative performance of the proposed Finemet-SMC-based generator. However, the analysis is subject to certain limitations that arise from idealised modelling assumptions. The electromagnetic, thermal and mechanical simulations are based on the material properties provided by the manufacturers, assuming uniform lamination quality, perfectly insulated laminations and defect-free fabrication. Consequently, manufacturing-induced phenomena, such as cutting-related degradation, tolerances in assembly, extra parasitic losses and imperfections in insulation, are not fully captured. Also, the thermal analysis is limited to largely steady-state operating conditions under idealised cooling effectiveness. The transient thermal response as well as the environmental variability and long-duration thermal cycling that would be most important for aerospace applications are not addressed. Thus, while the simulations indicate very strong potential for the proposed design, the absolute magnitude of predicted performance improvements should be interpreted cautiously until it is experimentally validated. Future work will be dedicated to experimental prototyping and validation to bridge the gap between numerical predictions and practical implementation. These plans include fabrication of Finemet-based stator assemblies using manufacturable lamination or ribbon-stacking techniques, followed by systematic core-loss and magnetic characterisations. Experimental investigations will also be performed with regard to key performance metrics, including power-speed characteristics, efficiency, torque ripple and thermal response under high-speed operation. Further studies will address manufacturing-induced losses, active cooling strategies and rotor-dynamic behaviour for long-term mechanical integrity and operational reliability. The experimental and technological investigations to be carried out are necessary to confirm the practical feasibility of the proposed generator and support its application in the next generation of electrified and hybrid aerospace propulsion.

## 8. Conclusion

This paper presents a next-generation high-speed radial-flux generator for aerospace applications, highlighting innovative winding optimisation and the use of advanced magnetic materials. The new design will implement Finemet in the stator, SMC in the rotor and Litz-wire windings to reduce AC losses and mitigate crucial limitations of conventional machines in terms of efficiency, thermal stability and structural weight. The resulting new topology offers improved electromagnetic compatibility and operational stability at high frequencies and high speeds. Improved thermal behaviour, based on intrinsic material properties as well as enhanced cooling strategies, allows the generator to operate within safe temperature limits even in very demanding aerospace environments. Minimising the core losses and overall mass of the system will considerably extend its applicability to next-generation avionic and onboard power systems. Additionally, the design will contribute to aviation sustainability goals by reducing energy losses, providing better power quality and minimising environmental impact. While these findings indeed reflect very strong potential for applications in electric and hybrid-electric propulsion systems, as well as for future aircraft electrification architectures, it should be underlined that the results presented here have been obtained using multiphysics simulations. In this sense, experimental prototyping and manufacturing validation are needed in order to fully confirm the predicted performance and evaluate the feasibility of large-scale production. Overall, this work sets a sound basis for the development of lightweight high-performance aerospace generators and supports continued research bridging simulation-driven design and practical implementation.

## Authors' contribution

Roby Mohajon – Research concept and design, writing the article. Abu Talha Haque Miah – Collection and/or assembly of data, data analysis and interpretation. Nur Mohammad – Critical revision of the article, final approval of the article.

## References

- Chebak, A., Viarouge, P. and Cros, J. (2010). Optimal Design of a High-Speed Slotless Permanent Magnet Synchronous Generator with Soft Magnetic Composite Stator Yoke and Rectifier Load. *Mathematics and Computers in Simulation, Modelling and Simulation of Electrical Machines, Converters and Power Systems*, 81, pp. 239–251. doi: 10.1016/j.matcom.2010.05.002
- Chen, T., Zhao, Z., Ming, L., Zhang, S., Ge, Y. and Wang, H. (2024). An Overview of Power Loss Calculation Methods for High-Frequency Litz Wires. *International Journal of Applied Electromagnetics and Mechanics*, 75, pp. 1–36. doi: 10.3233/JAE-230171
- Du, G., Li, N., Zhou, Q., Gao, W., Wang, L. and Pu, T. (2022). Multi-Physics Comparison of Surface-Mounted and Interior Permanent Magnet Synchronous Motor for High-Speed Applications. *Machines*, 10, p. 700. doi: 10.3390/machines10080700
- Du, Y., Gu, J., Zhang, H. and Hua, W. (2024). Reliability-Based Robust Optimization of High-Speed PM Synchronous Machine with Local Surrogate Model Strategy. *IEEE Transactions on Transportation Electrification*, 10, pp. 9679–9690. doi: 10.1109/TTE.2024.3360112
- Feng, L., Liu, W., Chen, X., Ding, Y., Yu, W. and Li, H. (2024). Design and Optimization of High-Speed Permanent Magnet Synchronous Motors. *Journal of Physics: Conference Series*, 2741, p. 012032. doi: 10.1088/1742-6596/2741/1/012032
- Fernando, N., Vakil, G., Arumugam, P., Amankwah, E., Gerada, C. and Bozhko, S. (2017). Impact of Soft Magnetic Material on Design of High-Speed Permanent-Magnet Machines. *IEEE Transactions on Industrial Electronics*, 64, pp. 2415–2423. doi: 10.1109/TIE.2016.2587815
- Gan, C., Zhu, M., Li, R. and Lu, B. (2024). Design and analysis of a high-speed PMSG with Litz wire winding technology. In: *2024 IEEE 10th International Power Electronics and Motion Control Conference (IPEMC2024-ECCE Asia)*, Chengdu, China. pp. 4442–4447. doi: 10.1109/IPEMC-ECCEAsia60879.2024.10567277
- Hamila, R., Chaabane, R., Askri, F., Jemni, A. and Nasrallah, S. (2017). Lattice Boltzmann Method for Heat Transfer Problems with Variable Thermal

- Conductivity. *International Journal of Heat and Technology*, 35, pp. 313–324. doi: 10.18280/ijht.350212
- Hu, X., Shi, G., Lai, Y., Wang, L. and Yu, J. (2023). Loss Calculation and Thermal Analysis of High-speed Magnetic Suspension Amorphous Motor. *International Journal of Fluid Power*, pp. 419–440. doi: 10.13052/ijfp.1439-9776.2431
- Huynh, C., Hawkins, L., Farahani, A. and McMullen, P. (2005). Design and Development of a Two-Megawatt, High Speed Permanent Magnet Alternator for Shipboard Application. *Naval Engineers Journal*, 117, pp. 23–29. doi: 10.1111/j.1559-3584.2005.tb00379.x
- IEC 60034-1:2022 | IEC (n.d). [WWW Document]. Available at: <https://webstore.iec.ch/en/publication/65446> [Accessed 18 Oct. 2025].
- IEEE SA - IEEE 1812-2014 (n.d). [WWW Document]. Available at: <https://standards.ieee.org/ieee/1812/4756/> [Accessed 18 Oct. 2025].
- Innovation | Carpenter Technology (n.d). [WWW Document]. Available at: <https://www.carpentertechnology.com/innovation> [Accessed 18 Oct. 2025].
- Ismagilov, F. R., Papini, L., Vavilov, V. E. and Gusakov, D. V. (2020). Design and Performance of a High-Speed Permanent Magnet Generator with Amorphous Alloy Magnetic Core for Aerospace Applications. *IEEE Transactions on Industrial Electronics*, 67, pp. 1750–1758. doi: 10.1109/TIE.2019.2905806
- Ismagilov, F. R., Varyukhin, A. N., Vavilov, V. E., Bekuzin, V. I. and Gusakov, D. V. (2021). System Approach to Electric Machines Development for Aviation Hybrid Propulsion Systems Under Economic Crisis. *IEEE Transactions on Aerospace and Electronic Systems*, 57, pp. 3768–3781. doi: 10.1109/TAES.2021.3082712
- Jiang, M., Cai, M., Zhou, J., Di, S., Li, X., Luo, Q. and Shen, B. (2023). Superior High-Frequency Performances of Fe-based Soft-Magnetic Nanocrystalline Alloys. *Materials Today Nano*, 22, p. 100307. doi: 10.1016/j.mtnano.2023.100307
- Kazeem Iyanda, F., Rezazadeh, H., Inc, M., Akgül, A., MujitabaBashiru, I., BilalHafeez, M. and Krawczuk, M. (2023). Numerical Simulation of Temperature Distribution of Heat Flow on Reservoir Tanks Connected in a Series. *Alexandria Engineering Journal*, 66, pp. 785–795. doi: 10.1016/j.aej.2022.10.062
- Liao, C., Bianchi, N. and Zhang, Z. (2024). Recent Developments and Trends in High-Performance PMSM for Aeronautical Applications. *Energies*, 17, p. 6199. doi: 10.3390/en17236199
- Liu, H., Xu, L. and Shanguan, M. (2011). Finite element method simulation of a high-speed wound-rotor synchronous machine. In: *2011 International Conference on Electrical Machines and Systems*, Beijing, China, pp. 1–4. doi: 10.1109/ICEMS.2011.6073611
- Metal powders | Höganäs (n.d). [WWW Document]. Available at: <https://www.hoganas.com/> [Accessed 18 Oct. 2025].
- Ning, Y., Liu, C., Jiang, R., Xu, J. and Zhu, S. (2012). A novel tangential radial hybrid excitation synchronous variable frequency aircraft generator. In: *2012 15th International Conference on Electrical Machines and Systems (ICEMS)*, Sapporo, Japan. pp. 1–5.
- Pasquinelli, M.G., Bolognesi, P., Guiducci, A., Nuzzo, S. and Galea, M. (2021). Design of a high-speed wound-field synchronous generator for the more electric aircraft. In: *2021 IEEE Workshop on Electrical Machines Design, Control and Diagnosis (WEMDCD)*, pp. 64–69. doi: 10.1109/WEMDCD51469.2021.9425625
- Qu, X., Xu, Z., Yao, J. and Zhang, F. (2023). Electromagnetic design and analysis of high speed permanent magnet motor with composite rotor. In: *2023 IEEE 6th International Electrical and Energy Conference (CIEEC)*. pp. 2593–2597. doi: 10.1109/CIEEC58067.2023.10166977
- Roy, R., Prabhakar, K. K. and Kumar, P. (2017). Core-Loss Calculation in Different Parts of Induction Motor. *IET Electric Power Applications*, 11, pp. 1664–1674. doi: 10.1049/iet-epa.2017.0369
- SAE International (n.d). Advancing mobility knowledge and solutions [WWW Document]. Available at: <https://www.sae.org/standards/content/arp4990> [Accessed 18 Oct. 2025].
- Shao, L., Navaratne, R., Popescu, M. and Liu, G. (2021). Design and Construction of Axial-Flux Permanent Magnet Motors for Electric Propulsion Applications—A Review. *IEEE Access*, pp. 1–1. doi: 10.1109/ACCESS.2021.3131000
- Shen, J., Qin, X. and Wang, Y. (2018). High-Speed Permanent Magnet Electrical Machines—Applications, Key Issues and Challenges. *CES Transactions on Electrical Machines and Systems*, 2, pp. 23–33. doi: 10.23919/TEMS.2018.8326449
- Sirimanna, S., Balachandran, T. and Haran, K. (2022). A Review on Magnet Loss Analysis, Validation, Design Considerations, and Reduction Strategies in Permanent Magnet Synchronous Motors. *Energies*, 15, p. 6116. doi: 10.3390/en15176116

- Taha, H., Barakat, G., Amara, Y. and Ghandour, M. (2023). An Overview of high-speed axial flux permanent magnets synchronous machines. In: S. Pierfederici, J. P. Martin, eds., Cham: Springer International Publishing, pp. 617–632. doi: 10.1007/978-3-031-24837-5\_46
- Talebi, D., Gardner, M. C., Sankarraman, S.V., Daniar, A. and Toliyat, H. A. (2021). Electromagnetic design characterization of a dual rotor axial flux motor for electric aircraft. In: *2021 IEEE International Electric Machines & Drives Conference (IEMDC)*, pp. 1–8. doi: 10.1109/IEMDC47953.2021.9449611
- Thangaraju, S. K., Munisamy, K. M. and Rajoo, S. (2022). Numerical Investigation on Cooling Performance of Oil Cooled PMSM Jacket Design with Vertical Straight Fin Design. *International Journal of Thermofluids*, 16, p. 100209. doi: 10.1016/j.ijft.2022.100209
- Tian, Y., Liang, S., Wang, F., Tian, J., Chen, K. and Liu, S. (2025). Analysis of Rotor Lamination Sleeve Loss in High-Speed Permanent Magnet Synchronous Motor. *Machines*, 13, p. 236. doi: 10.3390/machines13030236
- Torun, H. M. and Swaminathan, M. (2019). High-Dimensional Global Optimization Method for High-Frequency Electronic Design. *IEEE Transactions on Microwave Theory and Techniques*, 67, pp. 2128–2142. doi: 10.1109/TMTT.2019.2915298
- VAC - Advanced Magnetic Solutions | VAC (n.d). [WWW Document]. Available at <https://www.vacuumschmelze.com/> [Accessed 18 Oct. 2025].
- van der Geest, M., Polinder, H., Ferreira, J.A. and Zeilstra, D. (2015). Design and testing of a high-speed aerospace permanent magnet starter/generator. In: *2015 International Conference on Electrical Systems for Aircraft, Railway, Ship Propulsion and Road Vehicles (ESARS)*, pp. 1–6. doi: 10.1109/ESARS.2015.7101422
- Varyukhin, A. N., Ismagilov, F. R., Vavilov, V. Ye., Papini, L., Ayguzina, V. V. and Gordin, M. V. (2019). Design of 150-kVA 24,000-rpm high-speed permanent-magnet generator for more electric aircrafts. In: *2019 International Conference on Electrotechnical Complexes and Systems (ICOECS)*, Ufa, Russia. pp. 1–5. doi: 10.1109/ICOECS46375.2019.8949918
- Vavilov, V., Papini, L., Ismagilov, F., Song, S. and Ayguzina, V. (2019). High-Speed Permanent-Magnet Generator with Controlled Magnetic Flux for Aerospace Application. *International Review of Aerospace Engineering (IREASE)*, 12, pp. 290–301. doi: 10.15866/irease.v12i6.17748
- Vijayakumar, K., Karthikeyan, R., Sathishkumar, G. K. and Arumugam, R. (2008). Two dimensional magnetic and thermal analysis of high speed switched reluctance motor using soft magnetic composite material, Hyderabad, India. In: *TENCON 2008 - 2008 IEEE Region 10 Conference*, pp. 1–5. doi: 10.1109/TENCON.2008.4766454
- Wang, J., Yan, L., Gao, X. and Su, H. (2025). Electromagnetic Thermal Design and Analysis of Aviation Dual Three-Phase Permanent Magnet Machine. *IET Conference Proceedings*, 2024, pp. 2352–2357. doi: 10.1049/icp.2024.3382
- Wang, W., Fan, J., Li, C., Yu, Y., Wang, A., Li, S. and Liu, J. (2025). Low-Loss Soft Magnetic Materials and Their Application in Power Conversion: Progress and Perspective. *Energies*, 18, p. 482. doi: 10.3390/en18030482
- Wang, Y. X. and Wang, Y. (2011). Material Properties and Natural Frequency of Stator Core of Large Turbo-Generator. *Academy of Management Review*, 322, pp. 81–84. doi: 10.4028/www.scientific.net/amr.322.81
- Xing, Z., Wang, X. and Tian, M. (2017). Multi-field coupling analysis of high-speed permanent magnet machine, Sydney, NSW, Australia. In: *2017 20th International Conference on Electrical Machines and Systems (ICEMS)*, pp. 1–5. doi: 10.1109/ICEMS.2017.8056020
- Zhang, Z., Geng, W., Liu, Y. and Wang, C. (2019). Feasibility of a New Ironless-Stator Axial Flux Permanent Magnet Machine for Aircraft Electric Propulsion Application. *CES Transactions on Electrical Machines and Systems*, 3, pp. 30–38. doi: 10.30941/CESTEMS.2019.00005